Superconductivity of doped Ar@C_{60}†

Kenichi Yakigaya,[a] Atsuhiko Takeda,[ab] Yasunori Yokoyama,[ab] Seitaro Ito,[c] Takashi Miyazaki,[ab] Tomohiro Suetsuna,[a] Hidekazu Shimotani,[bd] Toru Kakiuchi,[e] Hiroshi Sawa,[f] Hidenori Takagi,[ac] Koichi Kitazawa[b] and Nita Dragoe*[g]

Received (in Montpellier, France) 17th January 2007, Accepted 3rd April 2007
First published as an Advance Article on the web 17th April 2007
DOI: 10.1039/b700726d

A substantial amount of endohedral fullerene, Ar@C_{60} (>1 mg), was successfully obtained by heat treatment of C_{60} powder under high pressure Ar atmosphere, followed by sequential HPLC separation. The isolation of pure Ar@C_{60} was demonstrated by TOF-MS, ^{13}C NMR spectroscopy and powder X-ray diffraction. We report here the synthesis of the first endohedral fullerene superconductors, K_3(Ar@C_{60}) and Rb_3(Ar@C_{60}) having critical temperatures of about 18 and 27 K, respectively. The decrease of T_c (ΔT_c) in both K_3(Ar@C_{60}) and Rb_3(Ar@C_{60}) compared with pristine compounds ($\Delta T_c > 1$ K and >2 K, respectively) is rather large, implying that the influence of encapsulated Ar atom on the C_{60} cage and therefore to the superconductivity of its derivatives, is more pronounced than expected. Indeed, synchrotron X-ray powder diffraction results showed, rather unexpectedly, that Ar@C_{60} and C_{60} have different unit cell parameters therefore different van der Waals radii.

Introduction

An interesting feature of fullerenes is the capability of capture of various atoms or molecules inside the cage. Endohedral C_{60}'s[1] usually encapsulate non-ionic-interacting elements such as nitrogen,[2] phosphorus[3] or noble gas atoms[4–6] and therefore are inert. No or little charge transfer takes place between the encapsulated atom and the cage, in marked contrast to metal endohedral fullerenes, for instance La- or Y-doped C_{82}.[7] In this sense, endohedral C_{60} compounds are considered as novel *van der Waals* derivatives.[8] Contrary to fullerene derivatives which manifest charge transfer thus modifying the structures,[9] the electronic[10] or magnetic properties,[11] the van der Waals derivatives' properties should be closely linked with those of empty fullerenes. We expect then that some of the unique characteristics of C_{60}, for example the superconductivity of doped C_{60},[12] are only modestly modified in "inert" endohedral compounds. In a recent letter we showed that the superconductivity is rather strongly affected by insertion of argon atoms inside the C_{60} cage.[13] This might be due to changes in the inter-cage distance. It was previously shown that the superconducting transition temperature T_c in doped C_{60} depended on the inter-cage distance, which was modified through intercalation of various metals.[14–16] Naively, the encapsulated atoms may lead to a decrease in T_c due to an isotopic-like effect. However, the influence of encapsulating atoms was well beyond this simple model despite that, traditionally, little changes are expected for a *van der Waals* system. A possible influence of the encapsulated atom is a change in the cage radius and/or a change in the intermolecular interactions. The phonons responsible for the superconductivity in the alkali doped C_{60} are high energy vibration modes of H_g symmetry, which may be affected by the insertion of an atom in the cage.[17] While the study of these materials is appealing, the difficulty in preparing pure endohedral fullerene samples has impeded a systematic research of this class of compounds. The synthesis of endohedral fullerenes is generally very difficult because of low yield and difficult synthetic conditions,[18] including the use of high pressure and high temperatures.[19,20] Ar@C_{60} was first synthesized by the Yale group[21] which showed that the HPLC enrichment of this compound is possible.[22] The similarity with the empty cage makes the purification of C_{60} endohedrals very difficult. Kr@C_{60} has been the first compound of this type to be purified, first at the 0.1 mg level[8] and later on a mg scale,[23,24] by a sequential HPLC procedure. By using a similar procedure, minute amounts of Xe@C_{60} have been also obtained.[25] We have optimized the conditions of separation of endohedrals by HPLC in terms of solvents, temperature and columns and found that the separation factor increases with size of the encapsulated atom. Based on this observation we expected that the separation of Ar@C_{60}, will be more difficult to achieve than that of Kr@C_{60}.

In order to test the superconductivity properties, relatively large amount of samples are required. We chose to study the

---

[a] *Department of Advanced Materials, University of Tokyo, Kashiwa, Japan. Fax: (+81)4-7136-3792; Tel: (+81)4-7136-3791*
[b] *Japan Science and Technology Agency (CREST), Kawaguchi, Japan*
[c] *The institute of Physics and Chemical research, RIKEN, Wako, Japan*
[d] *Institute for Materials Research, Tohoku University, Sendai, Japan*
[e] *Department of Materials Structure Science, The Graduate University for Advanced Studies, Tsukuba, Japan*
[f] *Institute of Materials structure Science, High Energy Accelerator Research Organization, Tsukuba, Japan*
[g] *Laboratoire d'Étude des Matériaux Hors Équilibre, (LEMHE-ICMMO), UMR 8182—CNRS, Université Paris Sud, 91405 Orsay, France*

† The HTML version of this article has been enhanced with colour images.

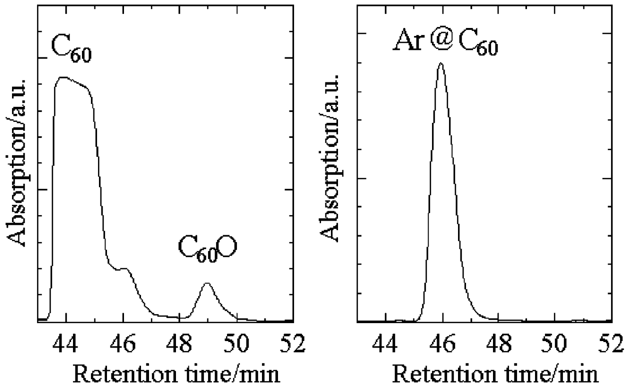

Fig. 1 Chromatogram of the first HPLC separation (left), and the eighth separation (right).

Ar derivative because it can be produced on a large scale by using a hot isostatic pressure device (HIP) whose pressure medium is argon gas. In this paper we discuss the separation and structural details of $Ar@C_{60}$ as well as the superconductivity of their potassium and rubidium intercalated derivatives (preliminary results were published recently in ref. 26).

Results and discussion

Separation and molecular structure

The chromatogram of the last cycle of the first HPLC separation by using Buckyprep columns is shown in the left panel of Fig. 1, and that of the eighth separation is shown in the right panel. The fractions eluting at 43.6, 45.1 and 48.2 min were identified as C_{60}, $Ar@C_{60}$ and $C_{60}O$, respectively. The comparable retention times for C_{60} and $Ar@C_{60}$ indicate their similar structures. After eight HPLC purifications, the second peak was collected. We estimated the separation factor of $Ar@C_{60}$ as 1.06, somewhat smaller than that of $Kr@C_{60}$ in the same condition (= 1.10). This tendency resembles the case for the 5PYE column where HPLC separation factors of $Ar@C_{60}$ and $Kr@C_{60}$ (with toluene as an eluent) are 1.04 and 1.09, respectively.[8,24]

Eventually, we obtained about 0.6 mg of $Ar@C_{60}$ with purity better than 98%. In successive experiments, we obtained additional 0.5 mg and 0.2 mg pure compounds. MALDI TOF mass spectra of the collected sample, $Ar@C_{60}$, showed a main peak at m/z 760, in agreement with the molecular weight of this endohedral. The experimental isotopic distribution agrees well with the theoretical one and only a trace of C_{60} signal was observed at m/z 720, testimony to the purity of the present $Ar@C_{60}$ sample.

Comparison of the ^{13}C NMR spectra for $Ar@C_{60}$ and C_{60}, Fig. 2, clearly demonstrates the effect of Ar on the electronic states of the C_{60} cage. For C_{60}, the resonance appears at 143.21 ppm (the bottom of Fig. 2), while, for $Ar@C_{60}$, a shift of the resonance to 143.38 ppm was observed. An argon atom inside C_{60} caused a downward shift of 0.17 ppm. The single resonance indicates that $Ar@C_{60}$ has the same symmetry as C_{60}, *i.e.* I_h. In other endohedral fullerenes, $Kr@C_{60}$ and $Xe@C_{60}$, the resonance is shifted downward by 0.39 ppm[8] and 0.96 ppm,[25] respectively, due to the effect of encapsulated atom on the C_{60} cage. It is likely that a larger change in the chemical shift is observed when a larger atom is encapsulated by a C_{60}, behavior similar to that of the separation factors in the HPLC experiments. This is consistent with a larger van der Waals interaction for a larger intercalated atom.

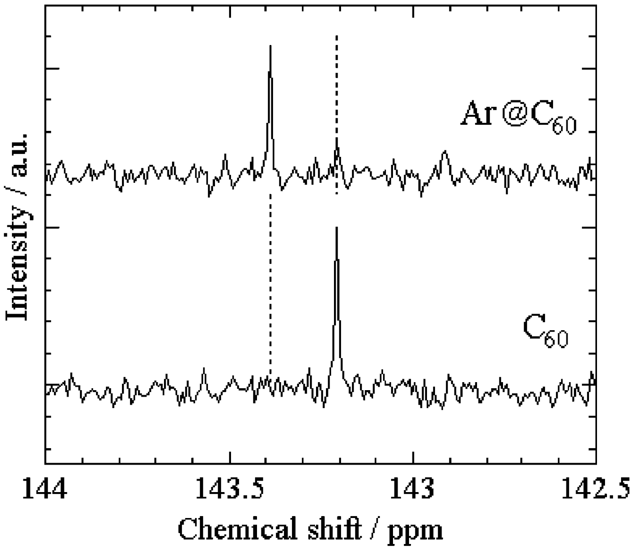

Fig. 2 ^{13}C NMR spectra of $Ar@C_{60}$ (top) and C_{60} (bottom), recorded in the same conditions (see Experimental section).

UV-Vis spectra of $Ar@C_{60}$ samples were measured for solutions in toluene at a concentration of about 0.02 mg ml^{-1}. There were no differences in the UV-Vis spectra (room temperature): both $Ar@C_{60}$ and C_{60} showed absorption bands at 283, 335, 406, 530, 540 and 598 nm. By considering that there is slight difference between UV-Vis spectra of $Kr@C_{60}$ and that of C_{60},[8] it is indicated that the effect of encapsulating an Ar atom is smaller than encapsulating a Kr atom.

The influence of the encapsulation of the atoms into the C_{60} cage to the vibrational properties of the molecule, essential to the superconductivity of these materials, can be inferred from IR and Raman spectra. We observed blueshifts of vibration modes lower than 510 cm^{-1} and the redshifts of vibrational modes higher than 770 cm^{-1}; the wavenumber shifts were about 4 cm^{-1} for $Ar@C_{60}$ compared to pristine C_{60} (Raman and IR experiments and *ab initio* calculations are submitted now).

Solid-state structural information

X-Ray diffraction data for C_{60}, $Ar@C_{60}$, K_3C_{60} and $K_3(Ar@C_{60})$, was obtained by powder diffraction experiments at SPring-8 synchrotron from 300 down to 100 K. Two sets of diffraction experiments, for two independent C_{60} and $Ar@C_{60}$ samples, were performed.

The peculiarities of solid-state structure and dynamics of C_{60} and related materials are well documented in a series of papers.[27–29] Rietveld[30] analysis allowed us to conclude that the solid-state behavior of $Ar@C_{60}$ is similar to that of C_{60}, that is, there is a rotational disorder at room temperature (for a detailed description for the C_{60} case see also ref. 29). An important point is that the rotational disorder at room temperature makes it possible to consider the cage as a spherical electronic distribution therefore its scattering factor can be expressed by a Bessel function.[31] This model explains why *h*00 peaks (*h* even) are not observed in room-temperature XRD patterns although they are allowed in a face centered cubic (FCC) structure. Rietveld analysis of C_{60} and Ar@C_{60} diffraction patterns obtained at 100 K and at room temperature, confirmed the absence of the (200) peak for the C_{60} measured at room temperature (all samples discussed here were prepared in identical conditions, annealed under dynamic vacuum). This is an indication, as the (200) peak appears if solvent is trapped into the structure or under external pressure,[32] that there is no detectable residual solvent remaining in the sample. In contrast, the Ar@C_{60} diffraction pattern clearly shows the (200) peak, this is due to the presence of the argon atom in the center of the fullerene cage, the 4a position in the $Fm\bar{3}m$ space group (Fig. 3).

The good fit obtained by using a Bessel function as the scattering factor for the cage confirms that the Ar@C_{60} is manifesting a similar behavior as C_{60}, in the solid state at room temperature. The fit is in good agreement both at room temperature when taking the C_{60} cage as a sphere and at low temperature when using the $Pa\bar{3}$ model, except for small tailings on (111) and (311) diffraction peaks.[33]

The refined fractional occupancy for the Ar atom was 97.8%.

Interestingly, the refined unit cell parameters for C_{60} and Ar@C_{60} were different (note that silicon was used as internal standard[34] so the obtained results have enough accuracy to detect the differences), Fig. 4. The Ar@C_{60} unit cell parameter is slightly larger at room temperature, but the decrease with lowering the temperature is larger than that of pristine C_{60}.

This striking result indicates an influence of the encapsulated atom to the lattice parameter and possibly to the cage dimension. We note that a previous single-crystal X-ray diffraction experiment of a sample having about 10% Kr@C_{60} in C_{60}, did not show any differences in the cage diameter compared to pristine C_{60}.[6] We could not perform an accurate analysis of the cage diameter from these data but the difference in the unit cell is undoubtful. The van der Waals radius of the cage is different for these two compounds and shows a different evolution with temperature.

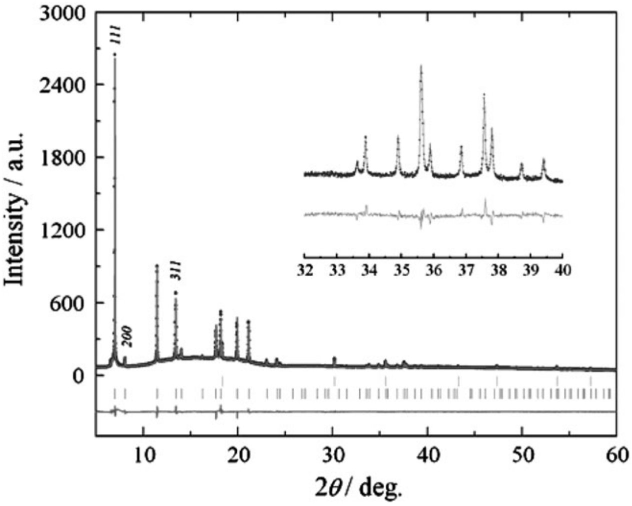

Fig. 3 Rietveld fit of Ar@C_{60} (0.5 mg) at room temperature; C_{60} approximated as a sphere of 3.55 Å radius (note the presence of the 200 line, the second diffraction peak, originating from the endohedral atom, see text). Silicon reference material, upper tickmarks, was used as internal standard. The inset is expanded diffraction pattern.

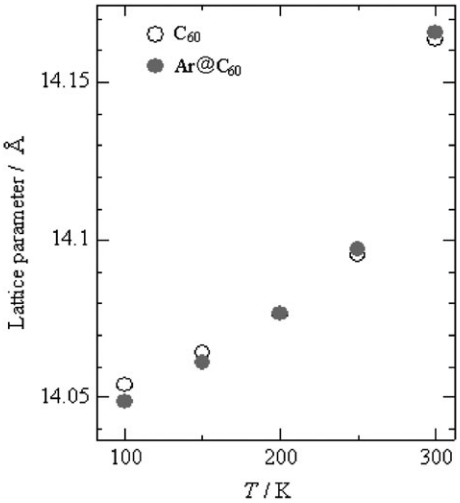

Fig. 4 Unit cell parameters as a function of temperature for C_{60} and Ar@C_{60}.

A low-temperature measurement (100 K) of C_{60} and Ar@C_{60}, was analyzed by the Rietveld method and the electronic distribution was calculated by using a maximum entropy method (MEM) with the software "Enigma".[35] Fig. 5 shows these results for C_{60} and Ar@C_{60} where structures corresponding to the frame of the C_{60} cage can be perceived. There is a high electron density region in the central part of the cage for Ar@C_{60}. By integrating the electronic density it was confirmed that an Ar atom is located in the center of the cage. This is the first 'direct' observation of the existence of an atom inside the C_{60} cage.

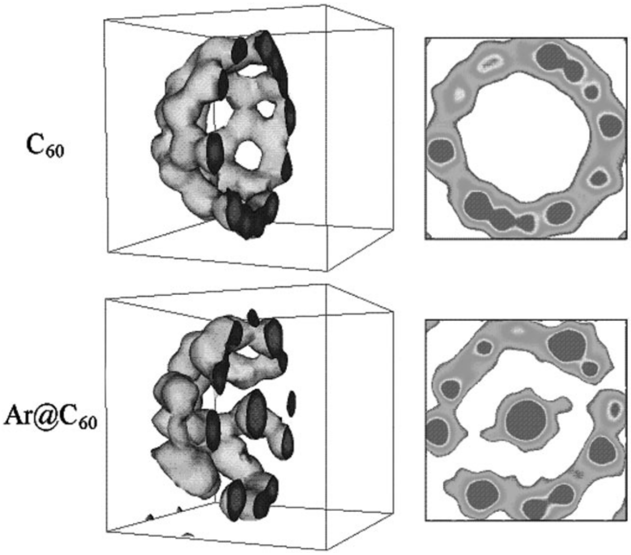

Fig. 5 Electronic density calculated by MEM for C_{60} and Ar@C_{60}, at 100 K. Right figures are cross-sections passing through the center of the frameworks in the left figures.

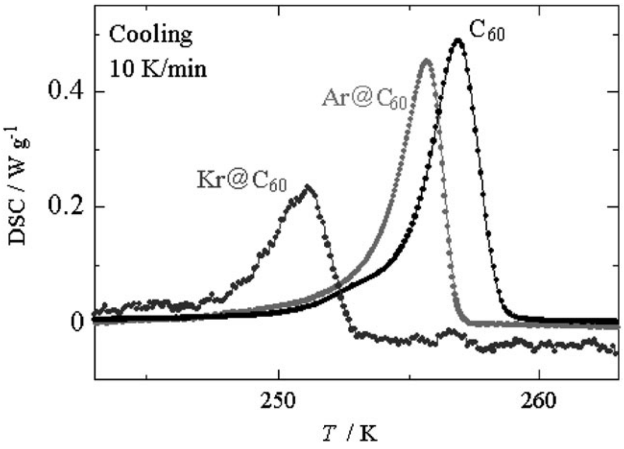

Fig. 6 DSC data for Ar@C_{60} compared with C_{60} and Kr@C_{60}. The amount of the sample is 0.205 mg, 0.9 mg and 0.05 mg, respectively.

An important point of the C_{60} dynamics is that the molecules rotate freely at the room temperature, and all molecules are equivalent. When the temperature decreases the rotation is gradually hindered. A phase transition related to this rotation takes place, manifested by a structural transition from FCC to a simple cubic (SC) lattice. The intermolecular distance decreases and the lattice parameter changes discontinuously at the transition temperature. Since the lattice parameters of C_{60} and Ar@C_{60} are different, it can be expected that the FCC to SC phase transition in Ar@C_{60} takes place at a different temperature. Fig. 6 shows the DSC measurement for C_{60}, Ar@C_{60} and, for comparison, Kr@C_{60}. Ar@C_{60} shows a phase transition similar to C_{60}, but with a transition temperature decreased by about 1.5 K. We speculate this decrease as the consequence of a *smaller cage* for the Ar@C_{60} compared to C_{60}. The decrease observed for the Kr@C_{60} transition temperature is even larger than for the argon case, suggesting that Kr@C_{60} has a *smaller* cage than Ar@C_{60}. We speculate that doping Kr@C_{60} will yield superconductors with critical temperatures *smaller* than for the Ar@C_{60}, see later. Note that, based on the transition temperatures, Ar and Kr compounds are rotating more easily than the empty cage.

Superconductivity

In order to have a good reproducibility we explored possible superconductivity by doping with potassium obtained by the thermal decomposition of KN_3.[36] The temperature dependent magnetization of K_3(Ar@C_{60}), obtained by KN_3 method, shows a clear diamagnetic signal below 17.6 K which was ascribed to superconductivity. The K_3C_{60} test sample, prepared in the same conditions, showed a T_c of 19.2 K.[13] The zero field signal corresponds to 11 and 13% of perfect diamagnetism for K_3(Ar@C_{60}) and K_3C_{60}, respectively (Fig. 7).

We found that the KN_3 method yields a better quality sample than the sublimation technique used in our previous experiment,[13] in terms of superconductivity properties,[37] and allows a better control of the stoichiometry, nevertheless there is a similar decrease in the critical temperatures for the superconductors obtained by the two methods.

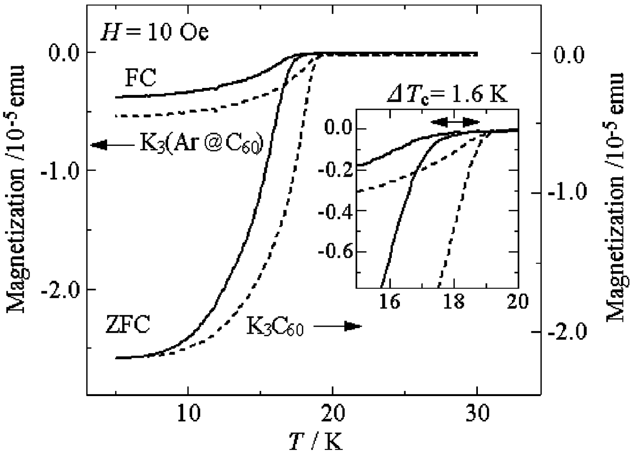

Fig. 7 Evidence for superconductivity at 17.6 K in K_3(Ar@C_{60}), compared to the signal of K_3C_{60} obtained in the same conditions (field 10 Oe, see text). The inset shows the expanded figure around T_c.

An important point to be considered when analyzing superconducting properties for these materials is that the decrease in the critical temperature, if this decrease is related to intrinsic properties for instance doping or isotopic effects, should be proportional to the critical temperature value. In this sense the T_c of rubidium doped endohedral compounds should give a larger T_c decrease than those of potassium. Rb_3C_{60} is a superconductor with a T_c of about 29.3 K and the T_c can reach 30 K for single crystals.[38] A Rb_3(Ar@C_{60}) sample together with Rb_3C_{60} prepared in identical conditions showed a clear depression of the critical temperature, larger than 2.5 K, Fig. 8. The zero field cooled signals for Rb_3(Ar@C_{60}) and Rb_3C_{60} were 11 and 31% of perfect diamagnetism, respectively.

The decrease of the critical temperature is significant, and is larger than for the potassium doped samples. In relative values the decrease is similar for the K and Rb doped compounds, that is about 8% of the T_c of the pristine C_{60} superconductors.

The XRD patterns of K_3C_{60} and K_3(Ar@C_{60}) (we measured the same samples in which the potassium doping was

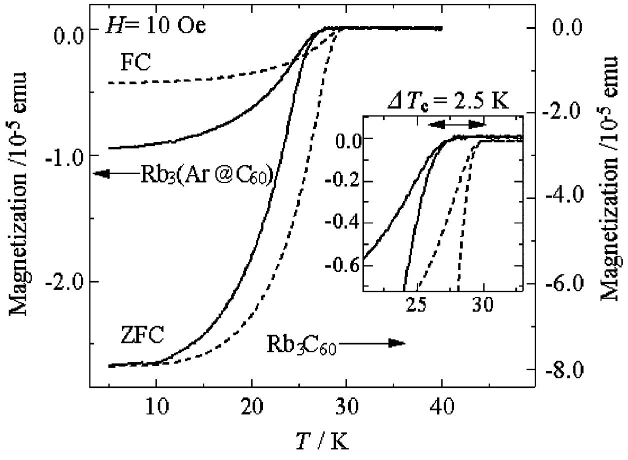

Fig. 8 Evidence for superconductivity at 26.8 K in Rb_3(Ar@C_{60}), compared to the signal of Rb_3C_{60} obtained in the same conditions (field 10 Oe, see text). The inset shows the expanded figure around T_c.

achieved by using KN_3) showed the typical peaks of FCC structures as well as several impurity peaks which could not be assigned. These impurities, showing low intensity peaks, do not belong to known phases involving K_xC_{60} compounds. The concentration of these impurities is under 10% assuming they are carbon based analogues.[39] We assume that these impurities do not intervene in the superconductivity properties because a similar pattern is present in both empty cage superconductors as in the $K_3(Ar@C_{60})$ ones. The data are not good enough to carry out quantitative Rietveld analysis, however we consider that the obtained unit cell parameters values are reliable: at room temperature they were 14.2743(5) Å for K_3C_{60} and 14.2035(3) Å for $K_3(Ar@C_{60})$. The expected unit cell parameter for the K_3C_{60} is 14.25 Å at room temperature.[40–42]

The precise value of the K_3C_{60} lattice parameter may be affected by a small error in the wavelength used (no internal standard was used for these samples) but the difference between the K_3C_{60} and $K_3(Ar@C_{60})$ is accurate. Another possibility for the slightly larger parameter for the K_3C_{60} than the expected value may be related to the presence of impurities, as observed by XRD experiments, or possibly with the reaction of $C_{60}{}^{3-}$ with traces of solvent trapped in the sample; this should affect both compounds in the same manner.

The slightly smaller unit cell parameter of $K_3(Ar@C_{60})$ than expected may be due to sample nonstoichiometry, inhomogeneities or possibly *to the effect of the encapsulated Ar atom* to the lattice. Lacking definitive structural information data one can not rule out that the differences in the T_c between K_xC_{60} and $K_x(Ar@C_{60})$ and Rb_xC_{60} and $Rb_x(Ar@C_{60})$, respectively, originate, at least partially, from nonstoichiometry or inhomogeneities in these samples.[43] We did not measure XRD data on the rubidium complex. However, there are several facts allowing us to propose that the T_c decrease is related to the influence of the encapsulated atom to the C_{60} cage. In support of this is the fact that doping pristine C_{60} by the same procedure and at the same level (<1 mg samples) showed critical temperatures consistent with previous results. Moreover, the change in the unit cell parameter of $K_3(Ar@C_{60})$ compared to K_3C_{60} is consistent with an *influence of the encapsulated atom to the unit cell parameter* of undoped C_{60}.

Concerning superconductivity, there are two main factors which can be considered when discussing the critical temperatures for these compounds: (i) phonon spectra distribution and (ii) density of states. For (i), the endohedral fullerenes may have different phonon spectra by considering simple mass effects or through the rattling mode vibration. For the first case, in a simple isotope shift model, assuming that argon atoms simply add an extra mass of 40 amu to the C_{60} cage, a T_c decrease of 0.5 K or less, should be observed.[44] The change in the phonon spectrum through the appearance of the rattling mode vibration would be in agreement with the shifts observed in our preliminary IR spectra.[45] However this contribution is difficult to estimate at this time and its influence should be rather small considering the small shifts and the low energy of the rattling mode. For (ii), changes in the density of states must be considered. It is unlikely, in such a van der Waals system where no or little charge transfer occurs, that the electronic density states at the Fermi level is directly modified. However, a subtle change in the *intermolecular interactions* triggered by the encapsulated atom should alter the band width. This change in the intermolecular interactions can be inferred from the slight but significant change in the unit cell parameter of $Ar@C_{60}$ compared to empty cage. It has been shown from the beginning of C_{60} research that T_c is almost linearly dependent of the lattice constant.[46] The critical temperature varies drastically with the unit cell parameters (about 25 K change for 0.5 Å difference), a dependence which was checked by high pressure XRD measurements.[47] In a crude approximation, taking the difference between the room-temperature lattice parameters of K_3C_{60} and $K_3(Ar@C_{60})$ and considering that the thermal expansion coefficients for these two compounds are the same, the expected critical temperature would be about 17 K. This value is in a rather good agreement with our results, considering the rough model, and it is equivalent to a unit cell parameter of K_3C_{60} at 0.33 GPa pressure.[47] This corresponds to about 10% decrease in the density of states. We therefore argue that the changes in the critical temperatures observed for these compounds are related to intrinsic properties of the endohedral superconductors rather than to sample preparation issues. Further work is required to determine the change in the superconductivity of endohedrals, particularly for larger atoms such as krypton and xenon where this effect should be more pronounced: these results show that encapsulation of inert atoms can generate additional channels to control the superconductivity of doped fullerenes.

Conclusions

We have reported the synthesis of relatively large amounts of pure $Ar@C_{60}$ (>1 mg, >98%) by using a hot isostatic pressure vessel and sequential HPLC purification. Powder XRD, MS, UV-Vis and NMR spectra of $Ar@C_{60}$ were discussed. With K and Rb doping, either with metallic potassium or with KN_3 or RbN_3 decomposition, we obtained the endohedral superconductors $K_3(Ar@C_{60})$ and $Rb_3(Ar@C_{60})$ with T_c of about 18 and 28 K, respectively. X-Ray diffraction data showed that the unit cell parameters of the endohedral derivative are different than those of pristine C_{60} and change with the temperature. We argued that the change of the unit cell parameters compared to pristine C_{60} is intimately linked with the intercage interactions in endohedral fullerenes and in their doped counterparts, giving rise to a substantial change of the T_c in the endohedral superconductors.

The existence of analogous endohedrals with high symmetry, including those with nitrogen, phosphorus and larger noble gas atoms, may prove a fruitful playground for the exploration of new superconductors and further developments in understanding the mechanism of superconductivity in fullerene materials.

Experimental

Synthesis was carried out using a HIP device Kobelco HHP100 which generates a maximum pressure of 500 MPa by using argon gas. In one batch, 2 g of C_{60} (>99.5%) was ground up together with 0.6 g of potassium cyanide (**CAUTION**: KCN is highly toxic; all manipulations must be done wearing a mask and gloves) to obtain a finely powdered mixture. This was put into a copper tube in the HIP vessel with Ar gas as the pressure medium and the temperature and the pressure in the vessel were maintained at 650 °C and 400 MPa. The experiment was conducted for 22 h. After cooling to room temperature, the resulting powder was ground in a mortar and extracted with toluene (the residual solid contains cyanides, careful manipulation and waste disposal must be ensured. We propose one example; the residual solid is put into a centrifuge tube. 1–2 cc of saturated NaCl solution is added and the tube is filled half full with water. This is sonicated and centrifuged. Then, the water is removed and put in a beaker. $FeCl_3$ solution is added to the water to form $Fe(Fe(CN)_6)$. Thus, cyanide is removed.).

Multi-stage HPLC was employed with the use of a large preparative Cosmosil Buckyprep [3-(1-pyrenyl)propyl] column (28 × 250 mm), an UV-Vis detector, recycling, and toluene as eluent at a flow rate of 50 mL min^{-1}. The sample was dissolved in toluene and 24 ml was injected at a time. A five-time-recycling was conducted for each injection. After recycling, unreacted C_{60} eluting at 43.8 min was separated, and the remainder was collected and re-injected. This procedure was repeated eight times. The UV-Vis spectrum was measured by a HITACHI U-4000 Recording spectrophotometer, at room temperature.

Matrix assisted laser desorption ionization time-of-flight mass spectrometry (MALDI-TOF-MS) was performed in negative ionization mode using a Bruker Reflex instrument with 9-nitroanthracene as the matrix. The main peak was assigned to Ar@C_{60} at 760 amu; two minor peaks ($<2\%$) were observed at 720 amu (C_{60}) and 736 amu ($C_{60}O$). The isotopic distribution is consistent with an Ar@C_{60} molecule.

The NMR spectrum was measured by a JEOL JNM-EX270 instrument running at a ^{13}C frequency of 67.5 MHz. The sample was dissolved in benzene-d_6. No relaxation agent was added. The benzene-d_6 triplet was used as a reference at 128.0 ppm. A line broadening of 0.28 Hz was applied when the free induction decay was processed.

Powder X-ray diffraction data were obtained at SPring-8 synchrotron by using a 0.1 nm wavelength obtained by Si(111) monochromators. The samples were mounted in 0.1 or 0.3 mm capillaries and analyzed in a Debye–Scherrer geometry with an ImagePlate detector; experiments of 10 min to 1 h exposure time were typically performed. Silicon standard reference material (SRM 640c) was used for C_{60} and Ar@C_{60}, it was mixed with the samples prior to filling the capillaries.

Thermal analysis was conducted with differential scanning calorimeter (DSC) 204 F1 Phoenix μ-sensor. The sample was put in the aluminium pan and the pan was sealed and pressed to obtain better thermal contact. The DSC data was measured between 110 and −50 °C using a 10 K min^{-1} scan rate.

For doping, Ar@C_{60} powder (0.5 mg) was sealed and heated at 250 °C in a quartz tube with a prescribed amount of potassium metal (K : Ar@C_{60} = 3 : 1) and decompressed He gas; we have processed a comparable amount of pure C_{60} powder using the same process. Additional experiments were performed with about 0.5 mg Ar@C_{60} dissolved in toluene encapsulated in a quartz tube together with 0.5 mg mL^{-1} KN_3/EtOH or RbN_3/EtOH. The ratio used for doping was C_{60} : K = 1 : 3.5; this ratio was determined as the optimum value for the superconductivity properties. The tube was heated to 600 °C to decompose the azides and then annealed under vacuum at 300 °C for 24 h. This procedure yields good superconductor samples synthesized even with only 0.15 mg of C_{60}.

The temperature dependent magnetization was measured by a commercial SQUID magnetometer (Quantum Design MPMS XL) under magnetic fields of H = 1 and 10 Oe.

Acknowledgements

We would like to thank Prof. R. James Cross (Yale University), Prof. Janice Musfeld (University of Tennessee, Knoxville) and Dr Fanica Cimpoesu (Institute of Physical Chemistry, Bucharest) for helpful suggestions.

References

1 (*a*) J. R. Heath, S. C. O'Brien, Q. Zhang, Y. Liu, R. F. Curl, H. W. Kroto, F. K. Tittel and R. E. Smalley, *J. Am. Chem. Soc.*, 1985, **107**, 7779; (*b*) T. Weiske, D. K. Böhme, J. Hrusák, W. Krätschmer and H. Schwarz, *Angew. Chem., Int. Ed. Engl.*, 1991, **30**, 884.
2 T. A. Murphy, T. Pawlik, A. Weidinger, M. Höhne, R. Alcala and J.-M. Spaeth, *Phys. Rev. Lett.*, 1996, **77**, 1075–1078.
3 J. A. Larsson, J. C. Greer, W. Harneit and A. Weidinger, *J. Chem. Phys.*, 2002, **116**, 7849–7854.
4 T. Weiske, D. K. Böhme, J. Hrusák, W. Krätschmer and H. Schwarz, *Angew. Chem., Int. Ed. Engl.*, 1991, **30**, 884–886.
5 K. A. Caldwell, D. E. Giblin, C. S. Hsu, D. Cox and M. L. Gross, *J. Am. Chem. Soc.*, 1991, **113**, 8519–8521.
6 H. M. Lee, M. M. Olmstead, T. Suetsuna, H. Shimotani, N. Dragoe, R. J. Cross, K. Kitazawa and A. L. Balch, *Chem. Commun.*, 2002, 1352–1353.
7 Y. Chai, T. Guo, C. Jin, R. E. Haufler, L. P. F. Chibante, J. Fure, L. Wang, J. M. Alford and R. E. Smalley, *J. Phys. Chem.*, 1991, **95**, 7564–7568.
8 K. Yamamoto, M. Saunders, A. Khong, R. J. Cross, M. Grayson, M. L. Gross, A. F. Benedetto and R. B. Weisman, *J. Am. Chem. Soc.*, 1999, **121**, 1591–1596.
9 M. Tanaka, M. Umeda, E. Nishibori, M. Sakata, Y. Saito, M. Ohno and H. Shinohara, *Nature*, 1995, **377**, 46–49.
10 L. Alvarez, T. Pichler, P. Georgi, T. Schwieger, H. Peisert, L. Dunsch, Z. Hu, M. Knupfer, J. Fink, M. S. Golden, P. Bressler and M. Mast, *Phys. Rev. B: Condens. Matter Mater. Phys.*, 2002, **66**, 35107.
11 *Endofullerenes*, ed. T. Akasaka and S. Nagase, Kluwer Academic, Dordrecht, 2002.
12 A. F. Hebard, M. J. Rosseinsky, R. C. Haddon, D. W. Murphy, S. H. Glarum, T. T. M. Palstra, A. P. Ramirez and A. R. Kortan, *Nature*, 1991, **350**, 600–601.
13 A. Takeda, Y. Yokoyama, S. Ito, T. Miyazaki, H. Shimotani, K. Yakigaya, T. Kakiuchi, H. Sawa, H. Takagi, K. Kitazawa and N. Dragoe, *Chem. Commun.*, 2006, 912–914.
14 M. J. Rosseinsky, A. P. Ramirez, S. H. Glarum, D. W. Murphy, R. C. Haddon, A. F. Hebard, T. T. M. Palstra, A. R. Kortan, S. M. Zahurak and A. V. Makhija, *Phys. Rev. Lett.*, 1991, **66**, 2830–2832.
15 K. Tanigaki, T. W. Ebbesen, S. Saito, J. Mizuki, J. S. Tsai, Y. Kubo and S. Kuroshima, *Nature*, 1991, **352**, 222–223.
16 M. Schluter, M. Lanoo, M. Needels, G. A. Baraff and D. Tomanek, *J. Phys. Chem. Solids*, 1992, **53**, 1473–1485.
17 (*a*) Y. Iwasa and T. Takenobu, *J. Phys.: Condens. Matter*, 2003, **15**, R495–R519; (*b*) O. Gunnarsson, *Rev. Mod. Phys.*, 1997, **69**, 575.
18 Recently, Komatsu and co-workers have succeeded in inserting hydrogen in fullerene in high yield by using a remarkable method of 'opening' the C_{60} cage: (*a*) Y. Murata, M. Murata and K. Komatsu, *J. Am. Chem. Soc.*, 2003, **125**, 7152; (*b*) K. Komatsu, M. Murata and Y. Murata, *Science*, 2005, **307**, 5707.
19 M. Saunders, H. A. Jiménez-Vázquez, R. J. Cross and R. J. Poreda, *Science*, 1993, **259**, 1428–1430.

20 M. Saunders, R. J. Cross, H. A. Jiménez-Vázquez, R. Shimshi and A. Khong, *Science*, 1996, **271**, 1693–1697.
21 M. Saunders, H. A. Jiménez-Vázquez, R. J. Cross, S. Mroczkowsk, M. L. Gross, D. E. Giblin and R. J. Poreda, *J. Am. Chem. Soc.*, 1994, **116**, 2193–2194.
22 B. A. DiCamillo, R. L. Hettich, G. Guiochon, R. N. Compton, M. Saunders, H. A. Jimenez-Vazquez, A. Khong and R. J. Cross, *J. Phys. Chem.*, 1996, **100**, 9197–9201.
23 T. Suetsuna, N. Dragoe, W. Harneit, A. Weidinger, H. Shimotani, S. Ito, H. Takagi and K. Kitazawa, *Chem. Eur. J.*, 2002, **8**, 5079–5083.
24 T. Suetsuna, N. Dragoe, H. Shimotani, A. Takeda, S. Ito, R. J. Cross, M. Saunders, H. Takagi and K. Kitazawa, *Fullerenes Nanotubes Carbon Nanostruct.*, 2002, **10**, 15–21.
25 M. S. Syamala, R. J. Cross and M. Saunders, *J. Am. Chem. Soc.*, 2002, **124**, 6216–6219.
26 A. Takeda, Y. Yokoyama, S. Ito, T. Miyazaki, H. Shimotani, K. Yakigaya, T. Kakiuchi, H. Sawa, H. Takagi, K. Kitazawa and N. Dragoe, *Chem. Commun.*, 2006, 912–914.
27 P. A. Heiney, J. E. Fischer, A. R. McGhie, W. J. Romanow, A. M. Denenstein, J. P. McCauley, Jr, A. B. Smith, III and D. E. Cox, *Phys. Rev. Lett.*, 1991, **67**, 1468.
28 A. B. Harris and R. Sachidanandam, *Phys. Rev. B: Condens. Matter Mater. Phys.*, 1992, **46**, 4944–4957.
29 P. A. Heiney, *J. Phys. Chem. Solids*, 1992, **53**, 1333–1352.
30 (*a*) H. M. Rietveld, *Acta Crystallogr.*, 1967, **22**, 151–152; (*b*) A. C. Larson and R. B. Von Dreele, *General Structure Analysis System (GSAS)*, Los Alamos National Laboratory Report LAUR, 2000, pp. 86–748; (*c*) B. H. Toby, *J. Appl. Crystallogr.*, 2001, **34**, 210–213.
31 W. Press and A. Huller, *Acta Crystallogr., Sect. A*, 1973, **29**, 252–256.
32 S. J. Duclos, K. Brister, R. C. Haddon, A. R. Kortan and F. A. Thiel, *Nature*, 1991, **351**, 380.
33 As often observed for C_{60} and related materials, low angle peak tailing,especially for 111 and 311 peaks, are indicative of king faults, a description is given in ref. 28.
34 SRM 640c, a = 0.54311946 ± 0.00000092 at 22.5 C, NIST, Gaithersburg, MD, USA. The wavelength determined by using this internal standard was 1.00134 Å.
35 H. Tanaka, M. Takata, E. Nishibori, K. Kato, T. Iishi and M. Sakata, *J. Appl. Crystallogr.*, 2002, **35**, 282.
36 We adopted a procedure similar to that described in: F. Bensebaa, B. Xiang and L. J. Kevan, *J. Phys. Chem.*, 1992, **96**, 6118–6120, which determines more precisely the amount of alkali metal used in the reaction. However, solid-state weighing and mixing of the reactants even by this method is not possible at 0.5 mg scale, we mixed solutions of the reactants then evaporated the solvents.
37 Since potassium can easily be distilled, the metal doping procedure is nevertheless better adapted to obtain purer samples when working with >5 mg samples.
38 S. H. Irons, J. Z. Liu, P. Klavins and R. N. Shelton, *Phys. Rev. B: Condens. Matter Mater. Phys.*, 1995, **52**, 15517–15521.
39 The presence of impurities is unavoidable, due to the small amount of the sample used and to the low solubility of fullerenes. In a 1 ml solution of toluene with a purity of 99.9%, the concentration of impurities may in fact be larger than that of the fullerene sample. The use of sublimed Ar@C_{60} is not possible with the amount of sample available.
40 P. W. Stephens, L. Mihaly, P. L. Lee, R. L. Whetten, S.-M. Huang, R. Kaner, F. Deiderich and K. Holczer, *Nature*, 1991, **352**, 632–634.
41 Y. Iwasa, S. Watanabe, T. Kaneyasu, T. Yasuda, T. Koda, M. Nagata and N. Mizutani, *J. Phys. Chem. Solids*, 1993, **54**, 1795–1800.
42 K. Tanigaki, J. Hirosawa, J. Mizuki and T. W. Ebessen, *Chem. Phys. Lett.*, 1993, **213**, 395–400.
43 As a matter of fact the first reports on the superconductivity properties of C_{60} derivatives quoted a critical temperature of 18 K for K_3C_{60}, and 28 to 28.6 K for Rb_3C_{60} found later to be 19.3 and 29.4 K, respectively. The first C_{60} superconductors, whose stoichiometries were unknown, showed low critical temperatures and rather small superconducting fractions (as low as 1%): it is possible that this was due to insufficient annealing which would convert a nonsuperconducting sample K_xC_{60} into C_{60} and superconducting K_3C_{60}).
44 Simply considering the isotopic effect, $\Delta T_c/T_c = 1 - (760/720)^\alpha$, gives −0.02 when taking $\alpha = 0.5$ predicted by the BCS theory.
45 The shifts observed in the vibrational spectra are in agreement with the localization of the argon atom on the attractive side of an interaction potential between the atom and the cage, this work is in progress and will be reported later.
46 G. Sparn, J. D. Thompson, R. L. Whetten, S. M. Huang, R. B. Kaner, F. Diederich, G. Grüner and K. Holczer, *Phys. Rev. Lett.*, 1992, **68**, 1228–1231.
47 The variation of the T_c with the pressure for K and Rb samples is similar, it was reported to be about −0.7 K $kbar^{-1}$: V. Buntar, in *Fullerenes, Chemistry, Physics and Technology*, ed. K. M. Kadish and R. S. Ruoff, Wiley Interscience, 2000, pp. 691–766.